Photon-number-resolved heralded-photon source for improved quantum key distribution

Tomoyuki Horikiri,[2,3] Yuishi Takeno,[2] Atsushi Yabushita,[4] and Takayoshi Kobayashi[1,3,4,5]
[1]*ICORP, JST, 4-1-8 Honcho, Kawaguchi, Saitama, Japan*
[2]*Department of Physics, Graduate School of Science, The University of Tokyo, 7-3-1 Hongo, Bunkyo, Tokyo 113-0033, Japan*
[3]*Institute of Laser Science and Department of Applied Physics and Chemistry, The University of Telecommunications, Chofu-ga-oka 1-5-1, Chofu, Tokyo 182-8585, Japan*
[4]*Department of Electrophysics, Faculty of Science, National Chiao Tung University, 1001 Ta Hsueh Road, Hsinchu, Taiwan 300*
[5]*Institute of Laser Engineering, Osaka University, Yamadagaoka 2-6, Suita, Osaka 565-0871, Japan*
(Received 18 May 2006; published 9 July 2007)

We have suppressed multiphoton probability of a heralded-photon source, which is vital for quantum key distribution with a higher secure key generation rate. It is accomplished by utilizing a practical photon-number-resolving detector for triggering resulting in an important step for improved practical quantum key distribution. Heralded-photon source and a practical photon-number-resolving detector capable of real-time processed multiphoton rejection are stably operable at room temperature and enable us to generate a secure key at a distance as long as an ideal single photon source is used.

DOI: 10.1103/PhysRevA.76.012306 PACS number(s): 03.67.Dd, 42.50.Ar

I. INTRODUCTION

Quantum key distribution (QKD) [1] is one of the most advanced fields in quantum information science in terms of practical applications. It is expected to bring unconditional security in classical communications. However, there are many difficulties with long distance secure communications [2]. One of them is the lack of single photon sources. Security of single photon based QKD is based on the most matured analysis in this field [3]. At present all the demonstrated single photon sources have finite and non-negligible multiphoton and zero photon emission probabilities which substantially degrade the secure key generation rate resulting in the reduction of overall bit rate of a QKD system.

Recently some proposals such as decoy state method [4–7] and Scarani-Acin-Ribordy-Gisin 2004 (SARG04) protocol [8] have enabled one to attain a high secure key generation rate and a long distance communication even with the use of a laser which has a substantially high multiphoton probability. However, it is still desirable to obtain a true single photon source in the decoy state method. (A combination of SARG04 and decoy state method has recently been discussed, and it was found to have lower performance than a combination of the Bennett-Brassard 1984 (BB84) protocol [1] and decoy state method. [9])

Here we consider a heralded-photon source (HPS) which utilizes spontaneous parametric down conversion (SPDC) [10–13]. When we adopt it to obtain single photon states, it is possible to decrease multiphoton probability by weak pumping of a nonlinear medium, which corresponds to a low mean photon number. However, there is a higher multiphoton probability in the case of relatively large mean photon number close to unity [6,14], because SPDC has a broader number distribution than a Poissonian case [15–17]. This is a drawback of HPS.

Here we adopt one solution to overcome the problem. SPDC is a process of simultaneous generation of a photon pair. Therefore after the separation of signal and idler by a polarizing beam splitter or a dichroic mirror, there are the same numbers of photons at the two exits and hence the photon number of the signal is revealed by counting that of the idler. Then the multiphoton signal can be rejected in the key generation process, resulting in the achivement of optimal key generation rate [14]. Here a time-multiplexed detector (TMD) [18,19] is utilized as a photon-number-resolving detector. Another advantage of the HPS is a reduced dark count probability by applying coincidence between a trigger detector and Bob's detectors. This makes longer distance communication possible [14,15].

II. PHOTON NUMBER DISTRIBUTION

Now let us consider the photon number distribution of SPDC with a mean photon number of μ. The output state of a single mode SPDC is given as follows [15,20]:

$$|\psi\rangle = \sum_{n=0}^{\infty} \sqrt{\frac{\mu^n}{(1+\mu)^{n+1}}} |n\rangle_s |n\rangle_i. \tag{1}$$

The photon number distribution of this state is thermal $\left[p(n)=\frac{\mu^n}{(1+\mu)^{1+n}}\right]$, however, it becomes to have the Poisson statistics in a highly multimode case [16,17]. The distribution cannot be sub-Poissonian in either case. A probability with which TMD detects an incoming signal as a single photon is given by

$$p_{\text{post}} = \frac{Nd_A}{1+\mu} + \sum_{n=1}^{\infty} \frac{\mu^n}{(1+\mu)^{1+n}} P(1|n). \tag{2}$$

Here

$$P(m|n) = \binom{N}{m} \sum_{j=0}^{m} (-1)^j \binom{m}{j} \left[(1-\eta_A) + \frac{(m-j)\eta_A}{N}\right]^n$$

[18] is the probability for m counts for n incident photons, N is the number of modes generated by the 50:50 beam splitters and optical fibers (here $N=4$), η_A is the detection efficiency of the single-photon detectors, and d_A is their dark

count probability. The photon number distribution after triggering is given as

$$p_{\text{post}}(n) = \begin{cases} \dfrac{1}{p_{\text{post}}} \dfrac{\mu^n}{(1+\mu)^n} P(1|n) & (n \geq 1) \\ \dfrac{1}{p_{\text{post}}} \dfrac{Nd_A}{1+\mu} & (n=0). \end{cases} \tag{3}$$

In case the pretriggering distribution is Poissonian, $\frac{\mu^n}{(1+\mu)^{1+n}}$ is replaced by $\frac{e^{-\mu}\mu^n}{n!}$. The resulting secure key generation rates are different between the two cases. The key rate is given by $R_{\text{decoy}}=q\{-Q_\mu f(E_\mu)H_2(E_\mu)+Q_1[1-H_2(e_1)]\}$ [6]. Here, $Q_1=Y_1 p_{\text{post}} p_{\text{post}}(1)$ is the gain of single photon states, while $Q_\mu=\Sigma_{i=0} Y_i p_{\text{post}} p_{\text{post}}(i)$ is the overall detection probability of a pulse with mean photon number μ [6,14]. In the conventional BB84 protocol, $q=\frac{1}{2}$, $H_2(e)$ is a binary entropy function, and $f(e)$ is a bidirection error correction efficiency. Y_n is Bob's detection probability conditioned that an n-photon pulse is sent from Alice. From the formula we can see that larger Q_1 and smaller Q_μ are desirable. A single (multi) photon probability of a thermal distribution is lower (higher) than that of a Poisson distribution in the case of the same mean photon number. Thus the key rate in the thermal distribution case is lower than that of the Poissonian one. If the TMD is a perfect photon number resolving detector, we can utilize only single photon signals. However, because the single photon probability of a Poisson distribution is higher ($Q_1^{\text{Pois}} > Q_1^{\text{thermal}}$), there is still a difference in their key rates. In both cases, it is possible to increase the key rate irrespective of the photon number distribution, if we can reject the multiphoton component.

III. EXPERIMENT

We measured the second-order correlation function to prove removal of a multiphoton for the improvement of the secure key generation rate. It is very difficult to precisely determine the photon number distribution by a direct measurement because of inaccurate evaluations of propagation losses and/or limited efficiencies of the detectors. Therefore measurements of photon statistics are performed widely by the second-order correlation function. The measurement of the correlation function in the case of the threshold detector was also demonstrated for comparison.

A. TMD

Figure 1 shows the block diagram of the apparatus of the measurement triggered by a TMD. A type II beta-barium borate (BBO) crystal was pumped by the second harmonics of a mode-locked Ti:sapphire laser (the repetition rate of 80 MHz, pulse width of 100 fs, and central wavelength of 800 nm). A collinear and frequency-degenerate pair of signal and idler was separated by a polarizing beam splitter. A reflected component (idler) was detected by a TMD to be utilized as a triggering signal. If and only if a single photon was detected, the measurement of the correlation function was triggered. Two cables after each coincidence detection system correspond to two temporal modes of the TMD.

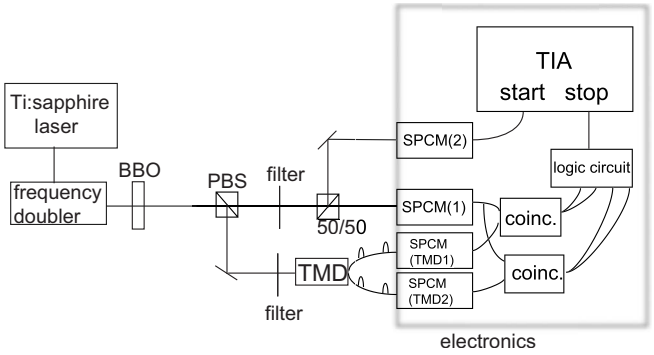

FIG. 1. Experimental setup for a TMD. BBO: type II beta-barium borate crystal, PBS: polarizing beam splitter, 50:50: half beam splitter, filter: interference filter, TIA: time interval analyzer, SPCM: single photon counting module (threshold detector), and coinc.: coincidence detection system (details are in text). Logic circuit: details are shown in the inset of Fig. 2.

Our detection system was composed in the following way to count the photon number and remove multiphoton components from the signals utilized for the key generation. The TMD consisted of optical fibers, 50:50 beam splitters, and two threshold detectors. By utilizing high efficiency (in the visible range) threshold detectors (Perkin Elmer, SPCM-AQR), resolution of photon number could be achieved. An incident pulse was divided into two paths by a 50:50 beam splitter. The arrival time shift due to the path length difference was set to be longer than the dead time of the detector. The two pulses were split again by a second 50:50 coupler which split pulses into two paths connected to two single photon detectors. Thus $N=4$ spatiotemporal modes were generated, and two photons in the incidence pulse were separated into two one-photon states with a certain probability (0.75 for $N=4$). Therefore the photon number was determined by counting the click number of the threshold detectors. We could obtain information of photon number of the signal mode due to the simultaneous generation of photon pairs. In this way we could achieve a higher secure key generation rate from this source [14].

The detection system sent accepting signals in case the single photon had been detected. To accept only single photon signals our detection system was configured using nuclear instruments module (NIM) signals converted from transistor-transistor-logic (TTL) pulses of single photon counting module (SPCM) outputs in the first part of the electronics (coincidence detection system in Fig. 1 and details are seen in Fig. 2). Coincidences between four TMD modes and a detector in signal mode [SPCM (1)] were taken. Then after NIM signals converted back into TTL signals, the coincidence signals between Bob's detector and four TMD modes were input to a logic circuit. This circuit was composed of XOR, NAND, and AND gates as shown in the inset of Fig. 2. An output TTL high level signal was generated if and only if one of four inputs had a TTL high level signal. Thus the detector in signal mode generated an output signal if the photon number of the trigger mode was measured to be one. Then the outputs were capable of being directly utilized for

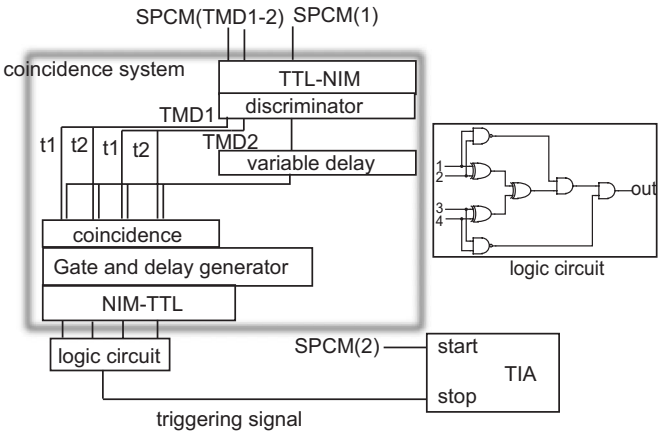

FIG. 2. The coincidence detection system and logic circuit (inset). A logic circuit rejects multiphoton signal. 1–4: coincidence signals between Bob's one detector and four TMD modes. Input signals are TTL. From the circuit a TTL high level signal is generated if and only if one of four inputs has a TTL high level signal.

QKD. Timing of the four coincidences was adjusted before the entrance of the logic circuit. To remove multiphoton signals we must carefully adjust it by using delay units (gate and delay generator in Fig. 2). Here the triggering signal is connected to the stop port of the time interval analyzer. Because the total response time of electronics was of the order of 100 ns, we used the stop port to save the module of delay units in the start port. (If we use the start port, another delay unit at the stop port is necessary.)

B. Threshold detector

Figure 3 shows the block diagram of the apparatus of the measurement triggered by a threshold detector. A type II beta-barium borate (BBO) crystal was pumped by the second harmonics of a mode-locked Ti:sapphire laser (repetition rate 80 MHz, pulse width 100 fs, and central wavelength 800 nm). The collinear frequency degenerate signal and idler were separated by a polarizing beam splitter. The reflected component (idler) was detected by a threshold detector and then utilized as a triggering signal. All the detected events

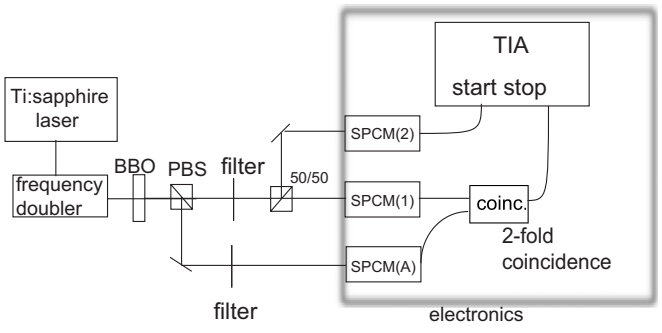

FIG. 3. Experimental setup for a threshold detector. BBO: type II beta-barium borate crystal, PBS: polarizing beam splitter, 50:50: half beam splitter, filter: interference filter, TIA: time interval analyzer, SPCM: single photon counting module (threshold detector), and coinc.: coincidence detection system (details are in Fig. 4).

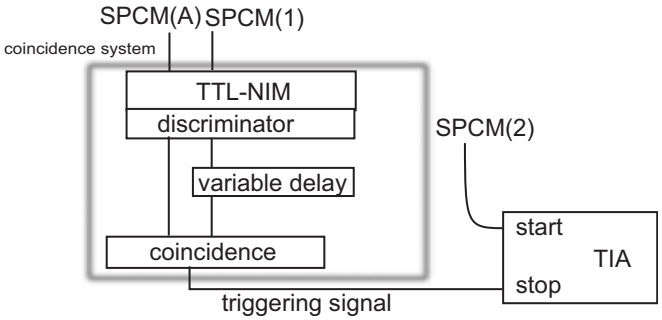

FIG. 4. The coincidence detection system for a threshold detector.

are accepted regardless of photon number and the measurement of correlation function was triggered. In Fig. 4, the electronics for the case of a threshold detector utilized for a trigger detector are shown. Here the electronics are much simpler than that of TMD. The triggering signal is the NIM signal (−1.3 V) in this case because there are no logic gates which need TTL inputs and the trigger level of the time interval analyzer can be negative.

C. Result

Figure 5 shows the results of the measurement triggered by the TMD (left) and by the threshold detector (right). Clearly, the central peaks are higher than the others in both cases. This measurement is different from usual measurement of correlation function on the point of the triggering [21,22].

The central peaks correspond to the events that two photon pairs are simultaneously generated by one pump pulse (here the effect of delays by electronics is subtracted), the idler two photons are detected as a single photon at a TMD or a threshold detector, signal two photons are separated by a 50:50 beam splitter and detected. On the other hand, for example, the right neighbor peaks correspond to the events that (i) two photon pairs are generated at different neighboring pulses (one pair exists at each pulse), the idler photon of

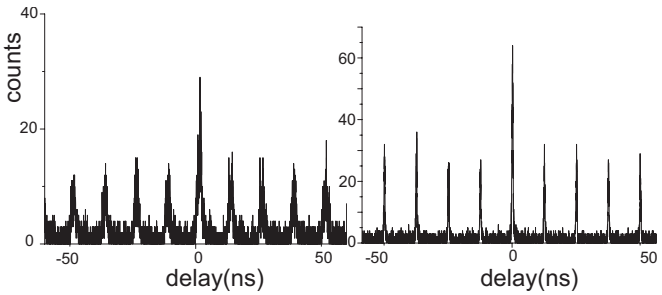

FIG. 5. Examples of the triggered measurements of correlation functions (bandwidth of interference filters=1.5 nm; a single mode fiber for the coupling of the signal): (left) by TMD and (right) by the threshold detector. The central peaks correspond to the events that two photon pairs are simultaneously generated by one pump pulse (here the effect of delays by electronics is subtracted). The noisy structure of TMD measurement is due to noise in the output voltage pulse from the logic circuit.

TABLE I. $I_{\text{reduction}}$, I_{TMD}, and I_{th} for four parameter settings. All fibers on the side of trigger detectors are multimode fibers.

		Threshold detector			TMD		
Coupling fibers for SPCM 1 and 2	$\Delta\lambda$	Central peak	Surrounding peaks	I_{th}	Central peak	Surrounding peaks	I_{TMD}
Single mode fiber	1.5 nm	1747	1008	1.73±0.05	1780	1157	1.54±0.07
	10 nm	346757	177291	1.96±0.01	333700	193671	1.72±0.02
Multimode fiber	1.5 nm	476788	319559	1.49±0.01	543362	410805	1.32±0.02
	10 nm	1996650	1392340	1.43±0.01	3353310	2637100	1.27±0.03

the latter pulse is detected, two signal photons (exist in neighboring pulses) are separated by a 50:50 beam splitter and detected, and (ii) one pair is generated at a former pulse and two pairs are generated at the latter pulse, the idler two photons of the latter pulse are detected as a single photon at a TMD or a threshold detector, one signal photon from the former pulse is detected and at least one of the signal photons at the latter pulse go to the other detector and are detected. Therefore the intensity ratio of the central peak-to-neighboring peaks is given as

$$I_{\text{TMD}} = p(2)\frac{1}{2}\eta^2 P(1|2) \Bigg/ \left[\left(p(1)\frac{\eta}{2}\right)^2 \eta_A + p(1)\frac{\eta}{2}p(2) \times\left(\frac{1}{2}\eta + \frac{1}{4}[1-(1-\eta)^2]P(1|2)\right)\right], \tag{4}$$

while a threshold detector is given as

$$I_{\text{th}} = p(2)\frac{1}{2}\eta^2[1-(1-\eta_A)^2] \Bigg/ \left[\left(p(1)\frac{\eta}{2}\right)^2 \eta_A + p(1)\frac{\eta}{2}p(2) \times\left(\frac{1}{2}\eta + \frac{1}{4}[1-(1-\eta)^2][1-(1-\eta_A)^2]\right)\right]. \tag{5}$$

Here we have assumed the detection efficiencies of two detectors after the 50:50 beam splitter are both equal to η and three photon probability is negligible. Since the first term in the denominators is much larger than the second term $[p(1) \gg p(2)$ under the low μ condition in the present experiment], the denominators of the two ratios $(I_{\text{TMD}}, I_{\text{th}})$ are nearly equal to each other. By using the following approximations,

$$I_{\text{TMD}} \approx p(2)\tfrac{1}{2}\eta^2 P(1|2) \Big/ \left[p(1)\tfrac{\eta}{2}\right]^2 \eta_A = \frac{2p(2)P(1|2)}{p(1)^2\eta_A},$$

$$I_{\text{th}} \approx p(2)\tfrac{1}{2}\eta^2[1-(1-\eta_A)^2] \Big/ \left[p(1)\tfrac{\eta}{2}\right]^2 \eta_A = \frac{2p(2)[1-(1-\eta_A)^2]}{p(1)^2\eta_A},$$

the ratio of I_{TMD} to I_{th} is shown to give the degree of removal of the two photon state

$$(I_{\text{reduction}} = I_{\text{TMD}}/I_{\text{th}} \approx P(1|2)/[1-(1-\eta_A)^2]).$$

Here $P(1|2)$ is a probability that a TMD detects a two photon as a single photon and $[1-(1-\eta_A)^2]$ is a detection probability of a threshold detector. Because photon number is not resolved by a threshold detector, all signals including at least one photon are used as a key. Thus $I_{\text{reduction}}$ is a probability that a TMD detects a two photon as a single photon normalized by that of a threshold detector and it becomes zero in an ideal case.

However, due to several possible imperfections such as inefficiencies, low coupling rates of detectors, and failure of mode separation in the TMD (0.25 for two photon in the four mode TMD), the resulting peak is not so low. Table I shows the ratios for the four cases of setting (bandwidth of interference filters=1.5 and 10 nm, coupling fibers for the signal are single mode and multimode fibers).

As mentioned above, the distribution becomes Poissonian in highly multimode cases. Both the conditional correlation functions (I_{TMD} and I_{th}) depend on the photon number distributions like an ordinary second order correlation function. However, we can predict the value of ratio $I_{\text{reduction}}$ is constant irrespective of the photon number statistics, as the experimental results shown in Table I verify. Figure 6(a) shows the calculated dependence of these three values on the trigger detection efficiency. Here the distribution is assumed to be Poissonian. However, $I_{\text{reduction}}$ does not change even if the distribution is changed. On the other hand, I_{TMD} and I_{th} depend on the type of distribution and a mean photon number. Thus they take different values as the spectral width and collected spatial mode are changed in Table I. If we assume that the detection efficiencies of the two trigger detectors are equal, the triggering efficiency is calculated as $\eta_A \approx 0.28$ from $I_{\text{reduction}}$. In this case, $P(1|2) \approx 0.42$ and $P(2|2) \approx 0.06$. [We show the dependence of these probabilities on the trigger detection efficiencies in Fig. 6(b). Since there is a finite probability of separation failure of 0.25 for $N=4$, $P(2|2) = 0.75$ even if a 100% efficiency trigger can be used. $P(1|2)$

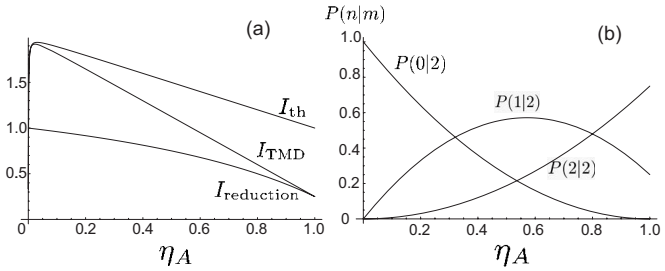

FIG. 6. Trigger detection efficiency dependence of (a) $I_{\text{reduction}}$, I_{TMD}, I_{th}, and (b) $P(n|m)$. We assume here the distribution is Poissonian and the mean photon number is 0.001. Though I_{TMD} and I_{th} depend on the distribution and mean photon number, $I_{\text{reduction}}$ is independent of them and coincides with the case for thermal distribution.

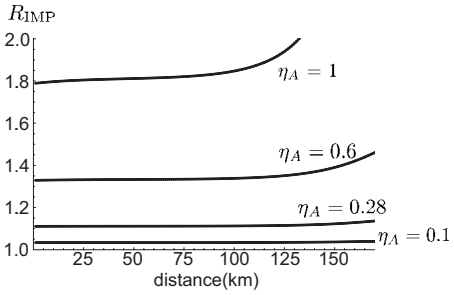

FIG. 7. Improvement in the key generation rate between the HPS-TMD scheme and HPS-threshold detector scheme R_{IMP}. $\eta_A = 1, 0.6, 0.28$, and 0.1 from top to bottom. The photon number distribution is assumed to be thermal. Right edge of the figure is 171 km which is the same maximum distance realized by using an ideal single photon source.

is a convex function, and ideally this is expected to be zero at a perfect trigger detection efficiency, but this takes 0.25 due to separation failure. $P(1|2)$ increases due to a misfire of a detector with a decrease in the trigger detection efficiency. Further decrease in the trigger detection efficiency reduces $P(1|2)$ resulting in the dominant contribution of $P(0|2)$.] Therefore even when a two photon arrives, the signal is regarded as a single photon in most of the cases. Therefore it is not possible to obtain legitimate single photon states in the present experiment. However, the secure key generation rate (hence the bit rate) can be improved by this slight multiphoton rejection as shown next.

IV. SECURE KEY GENERATION RATE

Here let us evaluate the degree of improvement in the secure key generation rate by the adoption of the TMD. Figure 7 shows the fractional improvement of secure key generation rate $R_{\mathrm{IMP}}=R_{\mathrm{decoy\ HPS-TMD}}/R_{\mathrm{decoyHPS-th}}$. Parameters for the calculations are taken from Ref. [23]. In the case of the perfect trigger detection ($\eta_A=1$), the degree of improvement is about 1.8 and rapidly increases from about 100 km. This is due to the fact that in the case of a perfect trigger detection we can utilize just single photon signals in most of the case. However, there is still a probability that we cannot reject two photon signals because of a failure of separation at TMD. Secure key generation rate of a true single photon source decreases more slowly than sources of thermal and Poisson photon number distributions. Thus R_{IMP} gradually increases with the transmission distance. However, as η_A decreases, the slope of key generation rate becomes steeper, and R_{IMP} is relatively reduced. About 10% improvement of the secure key generation rate by utilizing a TMD is attained in the case of $\eta_A=0.28$ under the present experimental condition. The rate of improvement is nearly constant in the range up to 171 km.

V. DISCUSSION

As shown above, good "single photon" nature could not have been obtained from our result for HPS-TMD. However, even if this low trigger detection efficiency is utilized, the maximum distance of secure key generation is as long as that of an ideal single photon source (171 km) due to the low dark count probability by coincidence detections. Some generation methods of a single photon state (for example, quantum dots, color centers, and single atoms [24]) have shown good sub-Poissonian statistics, hence they are promissing candidates for the quantum information technology. However, they are still not sufficient for practical applications because they have drawbacks such as a requirement of low temperature operation, difficulty in long optical fiber transmission resulting from a broad bandwidth, or necessity of high vacuum. On the other hand, a HPS is capable of being stably operated at room temperature for a very long term, and a TMD can also work at room temperature and the scale is so compact which is an advantage from a practical aspect. Therefore HPS-TMD is highly practical and ready for being utilized in a QKD system. (Other heralded photon sources have been demonstrated recently [25,26]. They utilized a cold atomic ensemble.) However, there is one limitation in the TMD system. We need to split the input pulse into four pulses which are temporally separated more than the dead time of detectors. Typical dead time of detectors is about 50 ns. Therefore the maximum repetition rate is limited below 20 MHz. Here we utilized four pulses (two temporal modes), hence it is limited below about a 10 MHz repetition rate, while the repetition rate of the pump laser is 80 MHz. The limitation of the QKD system with a HPS is determined not by a pump laser but a heralding detector. However, it does not become a serious problem in the present experiments' low μ conditions ($\ll 1$) and we could use 80 MHz repetition rate.

VI. SUMMARY

In summary, we have demonstrated multiphoton rejection of a heralded-photon source. Even though the present experiment has been a table-top experiment, our method can be applied for practical QKD, where a heralding signal is visible and the heralded signal is telecom wavelength.

ACKNOWLEDGMENT

We would like to thank D. Achilles, J. Franson, M. Fitch, S. Takeuchi, and I. Walmsley for their advice and F. Araoka and K. Nishimura for their help.

[1] C. H. Bennett and G. Brassard, in *Proceedings of IEEE International Conference on Computers, Systems, and Signal Processing, Bangalore, India* (IEEE, New York, 1984), p. 175.
[2] N. Gisin, G. Ribordy, W. Tittel, and H. Zbinden, Rev. Mod. Phys. **74**, 145 (2002).
[3] D. Gottesman, H.-K. Lo, N. Lütkenhaus, and J. Preskill, Quantum Inf. Comput. **5**, 325 (2004).
[4] W.-Y. Hwang, Phys. Rev. Lett. **91**, 057901 (2003).
[5] X.-B. Wang, Phys. Rev. Lett. **94**, 230503 (2005).
[6] H.-K. Lo, X. Ma, and K. Chen, Phys. Rev. Lett. **94**, 230504 (2005).
[7] X. Ma, B. Qi, Y. Zhao, and H. -K. Lo, Phys. Rev. A **72**, 012326 (2005).
[8] V. Scarani, A. Acin, G. Ribordy, and N. Gisin, Phys. Rev. Lett. **92**, 057901 (2004).
[9] Chi-Hang Fred Fung, K. Tamaki, and H.-K. Lo, Phys. Rev. A **73**, 012337 (2006).
[10] C. K. Hong and L. Mandel, Phys. Rev. Lett. **56**, 58 (1986).
[11] A. B. U'Ren, C. Silberhorn, K. Banaszek, and I. A. Walmsley, Phys. Rev. Lett. **93**, 093601 (2004).
[12] S. Takeuchi, R. Okamoto, and K. Sasaki, Appl. Opt. **43**, 5708 (2004).
[13] T. B. Pittman, B. C. Jacobs, and J. D. Franson, Opt. Commun. **246**, 545 (2005).
[14] T. Horikiri and T. Kobayashi, Phys. Rev. A **73**, 032331 (2006).
[15] N. Lütkenhaus, Phys. Rev. A **61**, 052304 (2000).
[16] H. D. Riedmatten, V. Scarani, I. Marcivic, A. Acin, W. Tittel, H. Zbinden, and N. Gisin, J. Mod. Opt. **51**, 1637 (2004).
[17] P. R. Tapster and J. G. Rarity, J. Mod. Opt. **45**, 595 (1998).
[18] M. J. Fitch, B. C. Jacobs, T. B. Pittman, and J. D. Franson, Phys. Rev. A **68**, 043814 (2003).
[19] D. Achilles, C. Silberhorn, C. Sliwa, K. Banazek, and I. A. Walmsley, Opt. Lett. **28**, 2387 (2003).
[20] D. F. Walls and G. J. Milburn, *Quantum Optics* (Springer, Berlin, 1995).
[21] P. Grangier, G. Roger, and A. Aspect, Europhys. Lett. **1**, 173 (1986).
[22] S. Fasel, O. Alibart, S. Tanzilli, P. Baldi, A. Beveratos, N. Gisin, and H. Zbinden, New J. Phys. **6**, 163 (2004).
[23] C. Gobby, Z. L. Yuan, and A. J. Shields, Appl. Phys. Lett. **84**, 3762 (2004).
[24] M. Hijlkema, B. Weber, H. P. Specht, S. C. Webster, A. Kuhn, and G. Rempe, Nat. Phys. **3**, 253 (2007).
[25] D. N. Matsukevich, T. Chaneliere, S. D. Jenkins, S.-Y. Lan, T. A. B. Kennedy, and A. Kuzmich, Phys. Rev. Lett. **97**, 013601 (2006).
[26] S. Chen, Y. A. Chen, T. Strassel, Z.-S. Yuan, B. Zhao, J. Schmiedmayer, and J.-W. Pan, Phys. Rev. Lett. **97**, 173004 (2006).